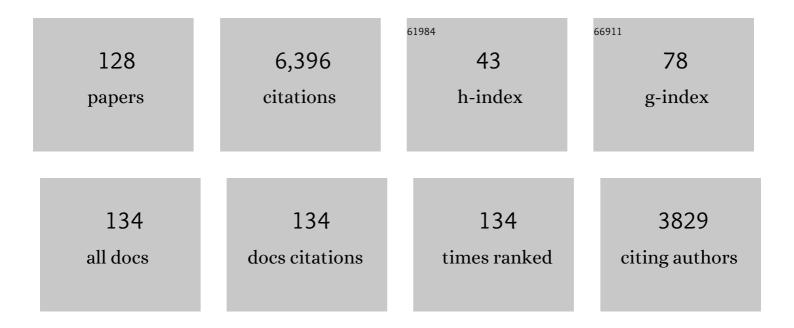
List of Publications by Year in descending order

Source: https://exaly.com/author-pdf/4508745/publications.pdf Version: 2024-02-01



#	Article	lF	CITATIONS
1	High-Density Electron Anions in a Nanoporous Single Crystal: [Ca24Al28O64]4+(4e-). Science, 2003, 301, 626-629.	12.6	744
2	Expanding frontiers in materials chemistry and physics with multiple anions. Nature Communications, 2018, 9, 772.	12.8	612
3	Light-induced conversion of an insulating refractory oxide into a persistent electronic conductor. Nature, 2002, 419, 462-465.	27.8	431
4	An oxyhydride of BaTiO3 exhibiting hydride exchange and electronic conductivity. Nature Materials, 2012, 11, 507-511.	27.5	251
5	Microporous Crystal 12CaO·7Al2O3 Encaging Abundant O- Radicals. Journal of the American Chemical Society, 2002, 124, 738-739.	13.7	225
6	Metallic State in a Limeâ^'Alumina Compound with Nanoporous Structure. Nano Letters, 2007, 7, 1138-1143.	9.1	208
7	Electron Localization and a Confined Electron Gas in Nanoporous Inorganic Electrides. Physical Review Letters, 2003, 91, 126401.	7.8	192
8	Field Emission of Electron Anions Clathrated in Subnanometer-Sized Cages in [Ca24Al28O64]4+(4e-). Advanced Materials, 2004, 16, 685-689.	21.0	175
9	Synthesis of a Room Temperature Stable 12CaO·7Al2O3 Electride from the Melt and Its Application as an Electron Field Emitter. Chemistry of Materials, 2006, 18, 1938-1944.	6.7	109
10	Hydride ions in oxide hosts hidden by hydroxide ions. Nature Communications, 2014, 5, 3515.	12.8	108
11	A Mixed Aqueous/Aprotic Sodium/Air Cell Using a NASICON Ceramic Separator. Journal of the Electrochemical Society, 2013, 160, A1467-A1472.	2.9	101
12	Thermodynamics and Kinetics of Hydroxide Ion Formation in 12CaO·7Al2O3. Journal of Physical Chemistry B, 2005, 109, 11900-11906.	2.6	91
13	Absolute emission current density of Oâ^' from 12CaOâ‹7Al2O3 crystal. Applied Physics Letters, 2002, 80, 4259-4261.	3.3	83
14	Maximum Incorporation of Oxygen Radicals, O- and O2-, into 12CaO·7Al2O3 with a Nanoporous Structure. Chemistry of Materials, 2003, 15, 1851-1854.	6.7	83
15	Intense thermal field electron emission from room-temperature stable electride. Applied Physics Letters, 2005, 87, 254103.	3.3	81
16	Grain Orientation Dependence of the PTCR Effect in Niobium-Doped Barium Titanate. Journal of the American Ceramic Society, 1996, 79, 1669-1672.	3.8	79
17	Crystal growth of Ca12Al14O33 by the floating zone method. Journal of Crystal Growth, 2002, 237-239, 801-805.	1.5	79
18	Partial oxidation of methane to syngas over promoted C12A7. Applied Catalysis A: General, 2004, 277, 239-246.	4.3	77

#	Article	IF	CITATIONS
19	Near-UV emitting diodes based on a transparent p–n junction composed of heteroepitaxially grown p-SrCu2O2 and n-Zno. Journal of Crystal Growth, 2002, 237-239, 496-502.	1.5	72
20	Fabrication of Highly Conductive 12CaO·7Al2O3 Thin Films Encaging Hydride Ions by Proton Implantation. Advanced Materials, 2003, 15, 1100-1103.	21.0	72
21	Simple and Efficient Fabrication of Room Temperature Stable Electride:Â Melt-Solidification and Glass Ceramics. Journal of the American Chemical Society, 2005, 127, 1370-1371.	13.7	71
22	Formation and Desorption of Oxygen Species in Nanoporous Crystal 12CaO·7Al2O3. Chemistry of Materials, 2004, 16, 104-110.	6.7	68
23	Czochralski Growth of 12CaO·7Al2O3Crystals. Crystal Growth and Design, 2006, 6, 1602-1605.	3.0	67
24	High-intensity atomic oxygen radical anion emission mechanism from 12CaO·7Al2O3 crystal surface. Surface Science, 2003, 527, 100-112.	1.9	65
25	Electron Carrier Generation in a Refractory Oxide 12CaO·7Al2O3by Heating in Reducing Atmosphere: Conversion from an Insulator to a Persistent Conductor. Journal of the American Ceramic Society, 2006, 89, 3294-3298.	3.8	65
26	Hopping and optical absorption of electrons in nano-porous crystal 12CaO·7Al2O3. Thin Solid Films, 2003, 445, 161-167.	1.8	64
27	Fabrication of room temperature-stable 12CaO·Â7Al2O3 electride: a review. Journal of Materials Science: Materials in Electronics, 2007, 18, 5-14.	2.2	63
28	Nanoporous Crystal 12CaO·7Al2O3: A Playground for Studies of Ultraviolet Optical Absorption of Negative Ions. Journal of Physical Chemistry B, 2007, 111, 1946-1956.	2.6	61
29	Mechanisms of oxygen ion diffusion in a nanoporous complex oxide12CaOâ^™7Al2O3. Physical Review B, 2006, 73, .	3.2	58
30	A High-Energy-Density Mixed-Aprotic-Aqueous Sodium-Air Cell with a Ceramic Separator and a Porous Carbon Electrode. Journal of the Electrochemical Society, 2015, 162, A1215-A1219.	2.9	58
31	Oxygen ion conduction in 12CaO·7Al2O3: O2â^' conduction mechanism and possibility of Oâ^' fast conductionâ^†. Solid State Ionics, 2009, 180, 550-555.	2.7	57
32	A liquid anode for rechargeable sodium-air batteries with low voltage gap and high safety. Nano Energy, 2018, 49, 574-579.	16.0	57
33	Hydride Ion as Photoelectron Donor in Microporous Crystal. Journal of the American Chemical Society, 2005, 127, 12454-12455.	13.7	56
34	Hydride Ion as a Two-Electron Donor in a Nanoporous Crystalline Semiconductor 12CaO·7Al2O3. Journal of Physical Chemistry B, 2005, 109, 23836-23842.	2.6	55
35	Formation of Oxygen Radicals in 12CaO·7Al2O3: Instability of Extraframework Oxide Ions and Uptake of Oxygen Gas. Journal of Physical Chemistry B, 2004, 108, 8920-8925.	2.6	53
36	Vibrational Dynamics and Oxygen Diffusion in a Nanoporous Oxide Ion Conductor 12CaO·7Al ₂ O ₃ Studied by ¹⁸ O Labeling and Micro-Raman Spectroscopy. Journal of Physical Chemistry C, 2007, 111, 14855-14861.	3.1	53

#	Article	IF	CITATIONS
37	Dual–phase Spinel MnCo 2 O 4 Nanocrystals with Nitrogen-doped Reduced Graphene Oxide as Potential Catalyst for Hybrid Na–Air Batteries. Electrochimica Acta, 2017, 244, 222-229.	5.2	52
38	Formation of inorganic electride thin films via site-selective extrusion by energetic inert gas ions. Journal of Applied Physics, 2005, 97, 023510.	2.5	51
39	Insights into Sodium Ion Transfer at the Na/NASICON Interface Improved by Uniaxial Compression. ACS Applied Energy Materials, 2019, 2, 2913-2920.	5.1	51
40	Thin film fabrication of nano-porous 12CaO·7Al2O3 crystal and its conversion into transparent conductive films by light illumination. Thin Solid Films, 2003, 445, 309-312.	1.8	50
41	Structural analysis and capacitive properties of carbon spheres prepared by hydrothermal carbonization. Advanced Powder Technology, 2017, 28, 884-889.	4.1	49
42	Field-Induced Current Modulation in Nanoporous Semiconductor, Electron-Doped 12CaO·7Al2O3. Chemistry of Materials, 2005, 17, 6311-6316.	6.7	45
43	Aqueous and Nonaqueous Sodium-Air Cells with Nanoporous Gold Cathode. Electrochimica Acta, 2015, 182, 809-814.	5.2	45
44	Formation of Potential Barrier Related to Grainâ€Boundary Character in Semiconducting Barium Titanate. Journal of the American Ceramic Society, 2000, 83, 2684-2688.	3.8	44
45	Photoinduced generation of electron anions in H-doped nanoporous oxide 12CaOâ^™7Al2O3: Toward an optically controlled formation of electrides. Applied Physics Letters, 2005, 86, 092101.	3.3	43
46	Superoxide Ion Encaged in Nanoporous Crystal 12CaO·7Al2O3 Studied by Continuous Wave and Pulsed Electron Paramagnetic Resonance. Journal of Physical Chemistry B, 2004, 108, 18557-18568.	2.6	41
47	Role of hydrogen atoms in the photoinduced formation of stable electron centers in H-doped12CaOâ^™7Al2O3. Physical Review B, 2006, 73, .	3.2	39
48	New functionalities in abundant element oxides: ubiquitous element strategy. Science and Technology of Advanced Materials, 2011, 12, 034303.	6.1	36
49	Effect of stability and diffusivity of extra-framework oxygen species on the formation of oxygen radicals in 12CaO�7AlO. Solid State Ionics, 2004, 173, 89-94.	2.7	35
50	A dense NASICON sheet prepared by tape-casting and low temperature sintering. Electrochimica Acta, 2018, 278, 176-181.	5.2	35
51	Functionalities of a Nanoporous Crystal 12CaO·7Al2O3Originating from the Incorporation of Active Anions. Bulletin of the Chemical Society of Japan, 2007, 80, 872-884.	3.2	34
52	Grain boundary structure in TiO ₂ -excess barium titanate. Journal of Materials Research, 1998, 13, 3449-3452.	2.6	32
53	Heavy doping of Hâ^' ion in 12CaO·7Al2O3. Journal of Solid State Chemistry, 2011, 184, 1428-1432.	2.9	31
54	Solid State Syntheses of 12SrO·7Al ₂ O ₃ and Formation of High Density Oxygen Radical Anions, O ^{â^'} and O ₂ ^{â^'} . Chemistry of Materials, 2008, 20, 5987-5996.	6.7	30

#	Article	IF	CITATIONS
55	Low temperature-densified NASICON-based ceramics promoted by Na2O-Nb2O5-P2O5 glass additive and spark plasma sintering. Solid State Ionics, 2018, 322, 54-60.	2.7	30
56	Grain boundary electrical barriers in positive temperature coefficient thermistors. Journal of Applied Physics, 1999, 86, 2909-2913.	2.5	29
57	Excess Oxygen in 12CaO·7Al2O3Studied by Thermogravimetric Analysis. Chemistry Letters, 2005, 34, 586-587.	1.3	28
58	Stabilization Mechanism of the Tetragonal Structure in a Hydrothermally Synthesized BaTiO ₃ Nanocrystal. Inorganic Chemistry, 2018, 57, 5413-5419.	4.0	28
59	C-axis oriented β″-alumina ceramics with anisotropic ionic conductivity prepared by spark plasma sintering. Solid State Ionics, 2014, 267, 22-26.	2.7	27
60	Electric Field Emission of High Density O[sup â^'] Ions from 12CaOâ‹7Al[sub 2]O[sub 3] Engineered to Incorporate Oxygen Radicals. Electrochemical and Solid-State Letters, 2002, 5, J13.	2.2	25
61	Direct Observation of the Double Schottky Barrier in Niobiumâ€Đoped Barium Titanate by the Charge ollection Current Method. Journal of the American Ceramic Society, 1998, 81, 1961-1963.	3.8	25
62	Anion Incorporation-induced Cage Deformation in 12CaO·7Al2O3Crystal. Chemistry Letters, 2007, 36, 902-903.	1.3	25
63	lodometric Determination of Electrons Incorporated into Cages in 12CaO·7Al ₂ O ₃ Crystals. Journal of Physical Chemistry C, 2010, 114, 15354-15357.	3.1	25
64	Active anion manipulation for emergence of active functions in the nanoporous crystal 12CaO·7Al2O3: a case study of abundant element strategy. Journal of Materials Science, 2007, 42, 1872-1883.	3.7	24
65	Hybrid Sodium–Air Cell with Na[FSA–C2C1im][FSA] Ionic Liquid Electrolyte. Electrochimica Acta, 2016, 218, 119-124.	5.2	24
66	Facile synthesis of nanorods of tetragonal barium titanate using ethylene glycol. Ceramics International, 2015, 41, 5581-5587.	4.8	23
67	Electronic insulator-conductor conversion in hydride ion-doped 12CaOâ^™7Al2O3 by electron-beam irradiation. Applied Physics Letters, 2005, 86, 022109.	3.3	22
68	Novel High-Energy-Density Rechargeable Hybrid Sodium–Air Cell with Acidic Electrolyte. ACS Applied Materials & Interfaces, 2018, 10, 23748-23756.	8.0	22
69	Reproducibility of O- Negative Ion Emission from C12A7 Crystal Surface. Japanese Journal of Applied Physics, 2002, 41, L530-L532.	1.5	20
70	Electron transport behaviors across single grain boundaries in n-type BaTiO3, SrTiO3 and ZnO. Journal of Materials Science, 2005, 40, 881-887.	3.7	19
71	Translucent Ceramics of 12CaO · 7Al ₂ O ₃ with Microporous Structure. Journal of Materials Research, 2002, 17, 1244-1247.	2.6	18
72	Natural nanostructures in ionic semiconductors. Microelectronic Engineering, 2004, 73-74, 620-626.	2.4	17

#	Article	IF	CITATIONS
73	Thermionic Electron Emission from a Mayenite Electride–Metallic Titanium Composite Cathode. Applied Physics Express, 2013, 6, 015802.	2.4	17
74	Liquid exfoliation graphene sheets as catalysts for hybrid sodium-air cells. Materials Letters, 2017, 187, 32-35.	2.6	17
75	Current–Voltage Characteristics of Σ1 Boundaries with and without Cobalt Ions in Niobiumâ€Doped SrTiO ₃ Bicrystals. Journal of the American Ceramic Society, 2000, 83, 1527-1529.	3.8	16
76	Localisation assisted by the lattice relaxation and the optical absorption of extra-framework electrons in 12CaO·Al2O3. Materials Science and Engineering C, 2005, 25, 722-726.	7.3	16
77	Kinetics of Electron Decay in Hydride Ion-Doped Mayenite. Journal of Physical Chemistry C, 2011, 115, 11003-11009.	3.1	16
78	Preparation of Nickel Nanoparticles by Direct Current Arc Discharge Method and Their Catalytic Application in Hybrid Na-Air Battery. Nanomaterials, 2018, 8, 684.	4.1	16
79	Investigation of the stability of NASICON-type solid electrolyte in neutral-alkaline aqueous solutions. Corrosion Science, 2020, 177, 109012.	6.6	15
80	Green apatites: hydride ions, electrons and their interconversion in the crystallographic channel. Physical Chemistry Chemical Physics, 2016, 18, 8186-8195.	2.8	14
81	Topotactic Synthesis of Mesoporous 12CaO·7Al ₂ O ₃ Mesocrystalline Microcubes toward Catalytic Ammonia Synthesis. Chemistry of Materials, 2018, 30, 4498-4502.	6.7	14
82	Reversible Electrochemical Insertion/Extraction of Magnesium Ion into/from Robust NASICON-Type Crystal Lattice in a Mg(BF ₄) ₂ -Based Electrolyte. ACS Applied Energy Materials, 2020, 3, 6824-6833.	5.1	14
83	Formation and quantification of peroxide anions in nanocages of 12CaO·7Al2O3. RSC Advances, 2013, 3, 18311.	3.6	13
84	Nanostructured titanium phosphates prepared via hydrothermal reaction and their electrochemical Li- and Na-ion intercalation properties. CrystEngComm, 2017, 19, 4551-4560.	2.6	13
85	Chlorideâ€Ionâ€Stabilized Strontium Mayenite: Expansion of Versatile Material Family. Journal of the American Ceramic Society, 2014, 97, 4037-4044.	3.8	12
86	Sn-Based Perovskite with a Wide Visible-Light Absorption Band Assisted by Hydride Doping. Chemistry of Materials, 2021, 33, 3631-3638.	6.7	12
87	Ferroelectricity of Dion–Jacobson layered perovskites CsNdNb ₂ O ₇ and RbNdNb ₂ O ₇ . Japanese Journal of Applied Physics, 2020, 59, SPPC04.	1.5	12
88	Humidity-Sensitive Electrical Conductivity in Ca[sub 12]Al[sub 14â^'x]Si[sub x]O[sub 32]Cl[sub 2+x] (0≤â‰9.4) Ceramics. Electrochemical and Solid-State Letters, 2009, 12, J11.	2.2	11
89	Field-assisted sustainable Oâ^' ion emission from fluorine-substituted 12CaO·7Al2O3 with improved thermal stability. Solid State Ionics, 2009, 180, 1113-1117.	2.7	11
90	Fabrication and transport properties of 12CaO·7Al ₂ O ₃ (C12A7) electride nanowire. Physica Status Solidi (A) Applications and Materials Science, 2008, 205, 2047-2051.	1.8	10

#	Article	IF	CITATIONS
91	Photonic materials utilizing naturally occurring nanostructures. Journal of Photochemistry and Photobiology A: Chemistry, 2004, 166, 141-147.	3.9	9
92	Controlling Defects to Achieve Reproducibly High Ionic Conductivity in Na ₃ SbS ₄ Solid Electrolytes. Chemistry of Materials, 2022, 34, 5634-5643.	6.7	9
93	Crystallization behavior of iron-based amorphous nanoparticles prepared sonochemically. Ultrasonics Sonochemistry, 2017, 35, 563-568.	8.2	8
94	Sodium titanium oxide bronze nanoparticles synthesized <i>via</i> concurrent reduction and Na ⁺ -doping into TiO ₂ (B). Nanoscale, 2019, 11, 1442-1450.	5.6	8
95	Variation of meso- and macroporous morphologies in resorcinol–formaldehyde (RF) gels tailored via a sol–gel process combined with soft-templating and phase separation. Journal of Sol-Gel Science and Technology, 2020, 95, 801-812.	2.4	8
96	Intense Atomic Oxygen Emission from Incandescent Zirconia. Journal of Physical Chemistry C, 2009, 113, 9436-9439.	3.1	7
97	Simultaneous Quantification of Hydride Ions and Electrons Incorporated in 12CaO·7Al ₂ O ₃ Cages by Deuterium-Labeled Volumetric Analysis. Journal of Physical Chemistry C, 2012, 116, 8747-8752.	3.1	7
98	Thermogravimetric Evolved Gas Analysis and Microscopic Elemental Mapping of the Solid Electrolyte Interphase on Silicon Incorporated in Free-Standing Porous Carbon Electrodes. Langmuir, 2019, 35, 12680-12688.	3.5	7
99	A highly conductive Na3V2(PO4)3 ceramic sheet prepared by tape-casting method. Electrochimica Acta, 2019, 305, 197-203.	5.2	7
100	Electronic Origin of Non-Zone-Center Phonon Condensation: Octahedral Rotation as a Case Study. Physical Review Letters, 2021, 127, 215701.	7.8	7
101	Gas sorption porosimetry for the evaluation of hard carbons as anodes for Li- and Na-ion batteries. Beilstein Journal of Nanotechnology, 2020, 11, 1217-1229.	2.8	6
102	Chemical bonding state at grain boundaries in BaTiO3 doped with a small amount of cation. Philosophical Magazine Letters, 1999, 79, 327-331.	1.2	5
103	Hopping and optical absorption of electrons in nano-porous crystal 12CaO·7Al2O3. Thin Solid Films, 2003, 445, 161-161.	1.8	4
104	Direct Characterization of Grainâ€Boundary Electrical Activity in Doped (Ba _{0.6} Sr _{0.4})TiO ₃ by Combined Imaging of Electronâ€Beamâ€Induced Current and Electronâ€Backscattered Diffraction. Journal of the American Ceramic Society, 2004, 87, 1153-1156.	3.8	4
105	Sustainable Thermionic O[sup â^'] Emission from Stoichiometric 12CaOâ‹7Al[sub 2]O[sub 3] with Nanoporous Crystal Structure. Journal of the Electrochemical Society, 2009, 156, G1.	2.9	4
106	Misorientation Dependence of Grain Boundary Resistivity in Nb-Doped Barium Titanate. Key Engineering Materials, 2000, 181-182, 51-54.	0.4	3
107	Proton conductive behaviors of Ba(Zn Nb1â^)O3â^'â^'(OH)2 studied by infrared spectroscopy. Journal of Solid State Chemistry, 2022, 308, 122913.	2.9	3
108	Grain Boundary Structure and Electrical Properties in Nb-Doped SrTiO ₃ Bicrystals. Key Engineering Materials, 2000, 181-182, 225-230.	0.4	2

#	Article	IF	CITATIONS
109	High-Density Electron Anions in a Nanoporous Single Crystal: [Ca24Al28O64]4+(4e-) ChemInform, 2003, 34, no.	0.0	2
110	Hydrothermal Synthesis of Tetragonal Barium Titanate Rod-like Crystal. Journal of the Society of Powder Technology, Japan, 2016, 53, 804-809.	0.1	2
111	Kinetic approach for the adsorption-photodecomposition properties of mesoporous silica-titania. Journal of the Ceramic Society of Japan, 2019, 127, 242-248.	1.1	2
112	Aging of starting solutions for nanoparticles synthesis with two different ultrasonication. Ultrasonics Sonochemistry, 2020, 67, 105142.	8.2	2
113	Natural nanostructures in ionic semiconductors. Microelectronic Engineering, 2004, 73-74, 620-626.	2.4	2
114	Synthesis of Hydride-Doped Perovskite Stannate with Visible Light Absorption Capability. Inorganic Chemistry, 2022, , .	4.0	2
115	Glass-ceramic route to NASICON-type Na Ti2(PO4)3 electrodes for Na-ion batteries. Ceramics International, 2022, 48, 24758-24764.	4.8	2
116	Photo-Induced Insulator-Semiconductor Transition in 12CaO·7Al2O3 (C12A7). Materials Research Society Symposia Proceedings, 2002, 747, 1.	0.1	1
117	Solid-state source of atomic oxygen for low-temperature oxidation processes: Application to pulsed laser deposition of TiO2:N films. Review of Scientific Instruments, 2012, 83, 023903.	1.3	1
118	Characterization of an AX Compound Derived from Ti2 SC MAX Phase. European Journal of Inorganic Chemistry, 2019, 2019, 2312-2317.	2.0	1
119	Mechanical and thermal properties of porous polyimide monoliths crosslinked with aromatic and aliphatic triamines. Journal of Sol-Gel Science and Technology, 0, , .	2.4	1
120	Light-Induced Conversion of an Insulating Refractory Oxide into a Persistent Electronic Conductor ChemInform, 2003, 34, no-no.	0.0	0
121	Fabrication of Highly Conductive 12CaO×7Al2O3 Thin Films Encaging Hydride lons by Proton Implantation ChemInform, 2003, 34, no.	0.0	0
122	Persistent Electronic Conduction in 12CaO7Al2O3 Thin Films Produced by Ar Ion Implantation: Selective Kick-Out Effect Leads to Electride Thin Films. Materials Research Society Symposia Proceedings, 2004, 811, 85.	0.1	0
123	Formation and Desorption of Oxygen Species in Nanoporous Crystal 12CaO×7Al2O3 ChemInform, 2004, 35, no.	0.0	0
124	Field Emission of Electron Anions Clathrated in Subnanometer-Sized Cages in [Ca24Al28O64]4+(4e-) ChemInform, 2004, 35, no.	0.0	0
125	12CaO·7Al2O3 (C12A7) ç³»ã®æ©Ÿèƒ½æ€§é€æ~Žå°Žé›»ä½"ææ−™. Hyomen Gijutsu/Journal of the Surface 641-646.	Finishing	Society of Jap
126	Structural Analysis of Mixed Anion Compounds. Nihon Kessho Gakkaishi, 2018, 60, 254-259.	0.0	0

#	Article	IF	CITATIONS
127	Sodium ion conduction in sodium lanthanum zirconate ceramics prepared by spark plasma sintering. Scripta Materialia, 2021, 200, 113887.	5.2	Ο
128	Revisiting Oxide-Based Sodium Ion Conductors for Next-Generation Batteries. Materia Japan, 2019, 58, 440-448.	0.1	0